Published April 1, 1996

Topology of Sphingolipid Galactosyltransferases in ER and Golgi: Transbilayer Movement of Monohexosyl Sphingolipids Is Required for Higher Glycosphingolipid Biosynthesis

Koert N.J. Burger,* Petra van der Bijl,*‡ and Gerrit van Meer*

*Department of Cell Biology, Faculty of Medicine, and ‡Department of Basic Sciences, Division of Biochemistry, Faculty of Veterinary Medicine, Institute of Biomembranes, Universiteit Utrecht, Utrecht, The Netherlands

Abstract. Glucosylceramide (GlcCer) is synthesized at the cytosolic surface of the Golgi complex while enzymes acting in late steps of glycosphingolipid biosynthesis have their active centers in the Golgi lumen. However, the topology of the "early" galactose-transferring enzymes is largely unknown. We used short-chain ceramides with either a 2-hydroxy fatty acid (HFA) or a normal fatty acid (NFA) to determine the topology of the galactosyltransferases involved in the formation of HFA- and NFA-galactosylceramide (GalCer), lactosylceramide (LacCer), and galabiosylceramide (Ga_2Cer).

Although the HFA-GalCer synthesizing activity colocalized with an ER marker, the other enzyme activities fractionated at the Golgi density of a sucrose gradient. In cell homogenates and permeabilized cells, newly synthesized short-chain GlcCer and GalCer were accessible to serum albumin, whereas LacCer and Ga_2Cer were protected. From this and from the results obtained after protease treatment, and after interfering with UDP-Gal import into the Golgi, we conclude that (*a*) GlcCer and NFA-GalCer are synthesized in the cytosolic leaflet, while LacCer and Ga_2Cer are synthesized in the lumenal leaflet of the Golgi. (*b*) HFA-GalCer is synthesized in the lumenal leaflet of the ER, but has rapid access to the cytosolic leaflet. (*c*) GlcCer, NFA-GalCer, and HFA-GalCer translocate from the cytosolic to the lumenal leaflet of the Golgi membrane. The transbilayer movement of GlcCer and NFA-GalCer in the Golgi complex is an absolute requirement for higher glycosphingolipid biosynthesis and for the cell surface expression of these monohexosyl sphingolipids.

GLYCOSPHINGOLIPIDS are universal membrane components of eukaryotic cells. They are enriched at the cell surface and in the lumen of endosomes and lysosomes (60). At the cell surface the glycosphingolipids not only exert functions in cell–cell interaction, cell–substrate interaction, and signal transduction, but are also used as receptors by bacteria, bacterial toxins, and viruses. Glycosphingolipids are a relatively minor constituent of most membranes, but a major component of myelin and of the apical plasma membrane of the polarized epithelial cells that line the gastrointestinal and urinary tract. In the latter tissues, glycosphingolipids play a structural role in rigidifying and protecting the cell surface. The apical plasma membrane of polarized epithelial cells is enriched in glycosphingolipids relative to the basolateral plasma membrane which contains less glycosphingolipids but more of the phospholipid phosphatidylcholine and the (sphingo)phospholipid sphingomyelin (SM).[1] Studies using epithelial cells in culture indicate that glycosphingolipids and phospholipids are sorted intracellularly before reaching the cell surface. Moreover, glycosphingolipids are thought to play a key role in the sorting of lipids and proteins to the appropriate plasma membrane domain (61). For our understanding of the molecular mechanisms that underlie biosynthesis, transport and sorting of gly-

Please address all correspondence to K. Burger, Department of Cell Biology, Universiteit Utrecht, AZU H02.314, 3584 CX Utrecht, The Netherlands, Tel: 31 30 2506480. Fax: 31 30 2541797. E-mail: K.N.J.Burger@med.ruu.nl

1. *Abbreviations used in this paper*: Ga_2Cer, galabiosylceramide, Gal α1-4 Gal β1-1 Cer; GalCer, galactosylceramide, Gal β1-1 Cer; GalT-1, UDP-galactose:ceramide galactosyltransferase; GalT-2, UDP-galactose:glucosylceramide galactosyltransferase; GalT-2b, UDP-galactose:galactosylceramide galactosyltransferase; GlcCer, glucosylceramide, Glc β1-1 Cer; GlcT, UDP-glucose:ceramide glucosyltransferase; GST, PAPS:galactosylceramide sulfotransferase; HFA, 2-hydroxy fatty acid; LacCer, lactosylceramide, Gal β1-4 Glc β1-1 Cer; M6P, mannose-6-phosphate; NFA, normal (nonhydroxy) fatty acid; N-Rh-PE, N-(lissamine rhodamine B sulfonyl) dioleoyl phosphatidylethanolamine; PAPS, 3′-phosphoadenosine 5′-phosphosulfate; SGalCer, sulfatide, HSO_3-3 Gal β1-1 Cer; SM, sphingomyelin.

Published April 1, 1996

cosphingolipids, it is essential to determine the intracellular location and the topology of the enzymes involved in glycosphingolipid biosynthesis.

Most glycosphingolipids, including virtually all gangliosides and globosides, are based on lactosylceramide (LacCer), which is formed by galactosylation of the monohexosyl sphingolipid, glucosylceramide (GlcCer). The second major monohexosyl sphingolipid is galactosylceramide (GalCer). In man, GalCer is particularly abundant in the epithelia of the intestine and kidney, and in the myelinating tissue of the nervous system. GalCer is the precursor of the gala-series of glycosphingolipids which includes galabiosylceramide (Ga_2Cer) and sulfatide (SGalCer). All sphingolipids are derived from ceramide (Cer), and though the final step in ceramide biosynthesis has not been localized yet, the last but one step, the formation of dihydroceramide occurs at the cytosolic surface of the ER (26, 35). After reaching the Golgi complex, where most enzymes involved in sphingolipid biosynthesis are localized, ceramide has access to both membrane leaflets by rapid spontaneous transbilayer movement because it lacks a polar headgroup. The ceramide receives a polar headgroup either at the lumenal or the cytosolic face of the Golgi membrane: the active center of SM-synthase is located in the lumen, and the formation of GlcCer by the ceramide glucosyltransferase (GlcT) is located at the cytosolic surface (15, 20, 28, 55). The cytosolic orientation of GlcT has direct consequences for the mechanism by which GlcCer is transported to the cell surface: at some stage during transport it must undergo transbilayer movement towards the lumenal or exoplasmic leaflet. Moreover, it has been shown that after conversion of GlcCer into LacCer by the galactosyltransferase GalT-2, subsequent steps in ganglioside biosynthesis occur in the lumenal leaflet of the Golgi (for review see 59). Thus, depending on the topology of GalT-2, ganglioside biosynthesis requires translocation of either GlcCer or LacCer to the lumenal leaflet of the Golgi membrane.

Conflicting results have been reported on the topology of GalT-2 (12, 16, 33, 55), but the most recent data (33) support a lumenal orientation of GalT-2 indicating that ganglioside biosynthesis depends on translocation of GlcCer to the lumenal leaflet of the Golgi membrane. One aim of the current study was to provide additional evidence for a lumenal orientation of GalT-2, and to compare the topology of GalT-2 with that of GalT-1, the enzyme responsible for the formation of GalCer. To this end, we extended an earlier study on the topology of SM-synthase and GlcT (28), and determined the intracellular location and topology of GalT-1 and GalT-2 in human liver-derived HepG2 cells. Our second aim was to determine the intracellular location and the topology of the enzymes involved in the biosynthesis of glycosphingolipids based on GalCer. For this, we switched to dog kidney MDCK II cells which express GalCer, Ga_2Cer, and SGalCer (11, 23, 39). Because GalCer and its derivatives often contain a 2-hydroxy fatty acid (HFA) instead of a nonhydroxy fatty acid (NFA), we characterized glycosphingolipid biosynthesis both using NFA- and HFA-ceramide analogues. Our data indicate that newly synthesized monohexosyl sphingolipids are present at the cytosolic surface of the ER and Golgi, and translocate from the cytosolic to the lumenal leaflet of the Golgi membrane in order to be used for higher glycosphingolipid biosynthesis.

Materials and Methods

Materials

UDP-Glc, UDP-Gal, 3′-phosphoadenosine 5′-phosphosulfate (PAPS), mannose-6-phosphate (M6P), egg phosphatidylcholine, and BSA (fraction V) were obtained from Sigma Chem. Co. (St. Louis, MO). Cell culture media and solutions were from Gibco (Glasgow, UK), and culture plastics from Costar Corp. (Cambridge, MA). Tunicamycin was from Boehringer Mannheim Corp. (Mannheim, FRG); pronase E (3,640 U/mg), saponin, and TLC-plates (Si60) from Merck (Darmstadt, FRG); CHAPS from Serva (Heidelberg, FRG); and Triton X-100 from Fluka (Buchs, FRG). *N*-6(7-nitro-2,1,3-benzoxadiazol-4-yl)-aminohexanoyl-ceramide (NBD-Cer) was purchased from Molecular Probes (Eugene, OR) and N-(lissamine rhodamine B sulfonyl) dioleoyl phosphatidylethanolamine (N-Rh-PE) was from Avanti Polar-Lipids (Birmingham, AL). NBD-analogues of SM, GlcCer, GalCer, and LacCer were synthesized from NBD-hexanoic acid as before (62). Hexanoyl NFA-[^{14}C]-Cer was synthesized by coupling D-erythro-sphingosine to [^{14}C]-hexanoic acid (specific activity 0.15 MBq/μmol), and hexanoyl HFA-[^{3}H]-Cer was synthesized by tritiating D-erythro-sphingosine and coupling the resulting D-[4,5-^{3}H]-sphinganine to D,L-2-hydroxy hexanoic acid; the natural D-stereoisomer of HFA-[^{3}H]-Cer (specific activity 201 MBq/μmol) was used after purification (58). HFA-[^{3}H]-GalCer was isolated from MDCK II cells incubated with HFA-[^{3}H]-Cer and purified by two-dimensional TLC. L,D-threo-PDMP (1-phenyl-2-decanoylamino-3-morpholino-1-propanol) was obtained from Matreya (Pleasant Gap, PA) and streptolysin-O was from Wellcome Diagnostics (Dartford, UK).

Cells

Cells were grown on plastic culture dishes, HepG2 cells in MEM with 10% FCS (53), CHO mutants Lec2 and Lec8 (Amer. Type Culture Collection, Rockville, MD) in MEM-α with 10% FCS (52) and D6P2T cells (5), a gift from S.E. Pfeiffer (Farmington, CT), in DMEM with 5% FCS. The medium was refreshed one day before the experiment, monolayers were 80–90% confluent. MDCK strain II cells (34), originally from K. Simons (Heidelberg), were grown in MEM with 5% FCS; confluent monolayers were used 3–4 d after seeding.

Determination of Sphingolipid Synthesis

Sphingolipid synthesis was determined using the hexanoyl lipids, NBD-Cer, NBD-GlcCer, NBD-GalCer, NFA-[^{14}C]-Cer, HFA-[^{3}H]-Cer, or HFA-[^{3}H]-GalCer as the precursor. Nucleotide sugars, PAPS and $MnCl_2$, were used at a concentration of 1, 0.3, and 2 mM, respectively. NBD-Cer was added in vesicles (62), the other ceramide analogues from 10-times concentrated stocks in 0.3% BSA (41).

Lipids were extracted according to Bligh and Dyer (8). All aqueous solutions were acidified to 10 mM acetic acid. When appropriate, KCl was added (0.44 wt/vol %) to force SGalCer into the chloroform phase; the aqueous phase was washed with chloroform, and applied to a SepPak C18 cartridge (Waters, Milford, MA) to recover any residual SGalCer present in the aqueous phase. Lipids were eluted from the column using chloroform/methanol/water (1/2.2/0.1, vol/vol) and methanol. Samples were dried under nitrogen, and applied to TLC-plates using chloroform/methanol (2/1, vol/vol) and in the case of samples containing SGalCer, chloroform/methanol/water (1/2.2/0.1, vol/vol). Lipids were separated by two-dimensional TLC on borate-treated TLC plates (29), using in the first dimension chloroform/methanol/ammonia (25%)/water, 65:35:4:4 (vol/vol), and in the second dimension chloroform/acetone/methanol/acetic acid/water, 50:20:10:10:5 (vol/vol). Radioactive lipids were detected by autoradiography after dipping the TLC plates in 0.4% PPO dissolved in 2-methylnaphtalene supplemented with 10% xylene (9); preflashed Kodak X-Omat S films were exposed for 2–4 d at −80°C. Radioactive lipid spots were scraped and quantified by liquid scintillation counting in a mixture of 0.3 ml Solulyte (Baker, Deventer, NL) and 3 ml Ultima Gold (Packard, Downers Grove, IL); background did not exceed 100 dpm [^{3}H] and 50 dpm [^{14}C]. Fluorescent lipid spots were quantified and corrected for background (1 pmol NBD-lipid or less) as described before (62).

Published April 1, 1996

Homogenization and Subfractionation

Cells were washed, scraped, and homogenized using a tight-fitting Dounce. A postnuclear supernatant (PNS) was prepared by a 10-min spin at 375 g_{max}. In experiments directly performed on a PNS, buffer A (120 mM K^+-glutamate, 15 mM KCl, 5 mM NaCl, 0.8 mM $CaCl_2$, 2 mM $MgCl_2$, 1.6 mM EGTA, 20 mM Hepes/KOH, pH 7.2) was used as the homogenization buffer. In subfractionation experiments, cells were allowed to swell in a low salt buffer (10 mM Hepes-NaOH, 15 mM KCl, 1.5 mM $MgCl_2$, pH 7.2; 750 μl per 9-cm dish) for 15 min on ice, scraped, and homogenized in the same buffer (53). The PNS from one 9-cm dish (750 μl, 1–1.5 mg protein) was layered on top of a linear sucrose gradient (0.7–1.5 M sucrose in 1 mM EDTA, 10 mM Hepes-NaOH, pH 7.2) and the 11-ml gradient was centrifuged (SW41, 3 h, 38,000 rpm, 4°C). N-Rh-PE was used as a plasma membrane marker (31): cells were incubated with 2 μM N-Rh-PE in HBSS-Hepes (HBSS, 10 mM Hepes-NaOH, pH 7.2) for 30 min at 0°C and washed with PBS (0°C). The rhodamine content of each gradient fraction was determined after lipid extraction and TLC (λ_{Ex} and λ_{Em} of 563 and 585 nm). Gradient fractions were analyzed by incubating 250 μl aliquots for 45 min at 37°C in the presence of $MnCl_2$ with 10 nmol NBD-Cer and UDP-Glc to monitor synthesis of SM and GlcCer; with 10 nmol NBD-Cer or 5 nmol NFA-[^{14}C]-Cer and UDP-Gal to monitor synthesis of SM and GalCer; with 0.6 nmol NBD-GlcCer and UDP-Gal to monitor synthesis of LacCer; with 50 pmol HFA-[^{3}H]-Cer, UDP-Glc, and UDP-Gal to monitor synthesis of HFA-SM, HFA-GlcCer, and HFA-GalCer; and with 4 pmol HFA-[^{3}H]-GalCer, UDP-Gal, and PAPS to monitor synthesis of HFA-Ga_2Cer and HFA-SGalCer. The distribution of calnexin, an ER marker, was determined by Western blotting using polyclonal antibodies (22), ^{125}I-protein–A, and phosphorimage analysis. Protein concentrations were determined using the BCA method (Pierce, Rockford, IL).

Sidedness in Permeabilized Cells

HepG2 monolayers were permeabilized using streptolysin-O (SLO) as described before (28), with some modifications: 1 U SLO (2 ml) was used per 6-cm culture dish, and cells were permeabilized in buffer A. Permeabilized and intact (control) cells were incubated at 10°C in 2 ml buffer A containing 26 nmol NBD-Cer and either UDP-Glc or UDP-Gal. After 3 h, the medium was replaced by 2 ml 1% (wt/vol) BSA in buffer A ($t = 0$) and the depletion of cellular NBD-lipids was followed at 10°C by renewing the BSA medium after 30 min, 1.5, 2.5, and 3.5 h. During the total incubation time of 6.5 h, a maximum of 30% of the cells detached. Before lipid analysis, the media were centrifuged (10 min, 375 g_{max}, 4°C) to pellet these cells. After the 3.5-h incubation with BSA, cells were scraped and analyzed together with the cell pellets. The sum of the fluorescence signals recovered from the synthesis medium, the BSA media, and the cells was set at 100%; the cell-associated fluorescence at each time point was then calculated by subtracting from this total the relative amount of fluorescence found in the media collected so far. It is important to note that only little additional NBD-lipid synthesis occurs during the BSA depletion (28).

Sidedness in Cell Homogenates

1 ml PNS (final volume; 1–2 mg protein) was incubated for 3 h at 10°C or for 30 min at 37°C with 26 nmol NBD-Cer or 75 pmol HFA-[^{3}H]-Cer, in the presence of UDP-Glc, UDP-Gal, $MnCl_2$, and (in some cases) PAPS. In a second set of experiments, higher glycosphingolipids were allowed to form for 30 min at 37°C, from 37 pmol HFA-[^{3}H]-GalCer or 2.2 nmol NBD-GalCer in the presence of UDP-Gal and PAPS, or from 2.2 nmol NBD-GlcCer and UDP-Gal. The sidedness of short-chain sphingolipids was determined using depletion by BSA or selective destruction of NBD-fluorescence by dithionite.

Depletion by BSA. 1 ml 10% (wt/vol) BSA in buffer A, with or without 0.2% (wt/vol) saponin, was added, and the sample incubated for 30 min on ice (unless stated otherwise). In another set of experiments, the depletion of short-chain sphingolipids by BSA was followed in time at 10°C. After BSA treatment, the sample (2 ml) was loaded on top of a 2-ml 0.4 M sucrose cushion (1 mM EDTA, 10 mM Hepes-NaOH, pH 7.2) and centrifuged (SW60, 30 min, 50,000 rpm, 4°C). About 15 min were required to transfer samples onto the sucrose cushions and start the centrifugation. The BSA-containing top fraction together with 300 μl of the sucrose interface, the remaining sucrose, and the membrane pellet were isolated, and their short-chain sphingolipid composition was analyzed. A phospholipid phosphorus determination indicated that saponin did not reduce the efficiency with which membranes were pelleted. The sucrose fraction never contained more than 15% of the short-chain sphingolipids, and was not specifically enriched in any of the sphingolipids. The relative amount of each sphingolipid present in the membrane pellet ("% protected") was calculated as a percentage of the total amount present in pellet and the BSA-containing top fraction.

Destruction of Fluorescence by Dithionite. 50 μl of a 1-M stock of sodium dithionite (37) was added, the samples incubated for 5 min on ice and the lipids extracted (8). The dithionite concentration required for selective destruction of NBD-lipid fluorescence should be determined empirically. It should be noted that the dithionite stock has a short shelf-life, and that its activity is only partially inhibited in a 1-phase Bligh and Dyer (8) lipid extract (also see reference 3).The relative amount of each sphingolipid present in the dithionite-treated sample (% protected) was calculated as a percentage of the total amount present in a control sample not treated with dithionite.

Protease Sensitivity

Pronase E treatment was performed as described (28) with some modifications. A Golgi-enriched membrane fraction was isolated at the interface between 1 ml 1.25 M sucrose and 1 ml 0.6 M sucrose, 10 mM EDTA in 10 mM Tris-maleic acid, pH 7.4 (SW60, 30 min, 50,000 rpm, 4°C). Aliquots of 100 μl (125 μg protein) were incubated with 25 μg pronase E (20 μl) for 0, 5, 10, 15, or 30 min at 37°C, after which 750 μl of ice-cold buffer (50 mM NaCl, 10 mM EDTA, 10 mM Tris-maleic acid, pH 7.4) containing 20 mg BSA/ml was added. The samples were overlaid on 3 ml 0.5 M sucrose, 10 mM Tris-maleic acid, pH 7.4, and the membranes pelleted (SW60, 30 min, 40,000 rpm, 4°C). Pellets were resuspended in 500 μl 250 mM sucrose, 10 mM Tris-maleic acid, pH 7.4 (0°C). Sphingolipid synthesis was assayed in the presence of $MnCl_2$ for 45 min at 37°C, with 13 nmol NBD-Cer and either UDP-Glc or UDP-Gal, or with 0.6 nmol NBD-GlcCer and UDP-Gal, or with 164 pmol HFA-[^{3}H]-Cer, and both UDP-Gal and UDP-Glc. The pronase activity is not completely neutralized by the addition of the BSA-containing buffer; at 0-min pronase treatment, the activity of the pronase sensitive sphingolipid synthesizing enzymes was reduced by ~25% as compared to samples not treated with pronase. In another set of experiments, the membrane-pelleting step was omitted and protease treatment and sphingolipid synthesis occurred simultaneously: a Golgi-ER membrane fraction was isolated from the PNS of MDCK II cells at the interface between 1.5 and 0.6 M sucrose. Aliquots were preincubated at 37°C for 15 min with pronase E in the absence or presence of detergent. HFA-[^{3}H]-Cer and nucleotide sugars were added (see above), and the samples were further incubated for 30 min at 37°C.

Drug Incubations

Brefeldin A. BFA, dissolved in ethanol (100 μg/ml), was added to the growth medium to a final concentration of 1 μg/ml (identical results were obtained at 5 μg/ml), and the cells were left in the incubator for 1 h. Ethanol was added to the control cells.

PDMP. L,D-threo-PDMP was added from 200-times concentrated stock solutions in ethanol, 5 μl/ml to a final concentration of 0 μM (only ethanol added), 5 μM, or 50 μM (in HBSS-Hepes). After a 30-min preincubation with PDMP at 10°C (1 ml), HFA-[^{3}H]-Cer (82 pmol per 3-cm dish), NBD-Cer (10 nmol), or NFA-[^{14}C]-Cer (8 nmol) was added and the dishes incubated for 1.5 h at 37°C in the presence of PDMP. Cells and medium were analyzed together.

Tunicamycin. Tunicamycin was added from a stock of 1 mg/ml 10 mM NaOH in distilled water. A PNS (250 μl 1–2 mg protein/ml) was incubated for 30 min at 37°C in the presence of tunicamycin and $MnCl_2$, with 10 nmol NBD-Cer and either UDP-Glc or UDP-Gal, with 0.5 nmol NBD-GlcCer and UDP-Gal, or with 50 pmol HFA-[^{3}H]-Cer and both UDP-Glc and UDP-Gal.

Miscellaneous Procedures

BSA Depletion of Lipid Vesicles. Large unilamellar egg phosphatidylcholine vesicles containing 0.3 mol% N-Rh-PE and a total of 1 mol% of short-chain sphingolipids were prepared in HBSS-Hepes by extrusion of freeze-thawed multilamellar vesicles through two stacked polycarbonate filters (pore size 200 nm; Nuclepore Corp., Pleasanton, CA) as described (36). The vesicles were incubated with various concentrations of BSA for 30 min at 20°C, and separated from the (BSA-containing) medium by flotation: 0.1 ml was mixed with 1.4 ml 53.5% (wt/vol) sucrose (10 mM Hepes-NaOH, pH 7.4), overlayered with 2 ml 20% sucrose (10 mM Hepes-NaOH, pH 7.4) and 0.5 ml 10 mM Hepes-NaOH (pH 7.4), and cen-

Published April 1, 1996

trifuged (SW60, 2 h, 50,000 rpm, 4°C). Subsequently, five fractions were isolated from top to bottom, with volumes of 250, 500, 1,500, 500, and 1,250 μl. The vesicles were efficiently separated from the (BSA-containing) medium collected in fractions 4 and 5: fractions 1–5 contained 11.5 ± 10.1, 69.9 ± 3.9, 14.2 ± 4.4, 2.0 ± 0.6, and 2.5 ± 1.6% of the nonexchangeable (vesicle) marker N-Rh-PE (σ_{n-1} with $n = 3$). Moreover, when an NBD-Cer/BSA mixture was centrifuged and subfractionated as described above, over 95% of the NBD-Cer was recovered in fractions 4 and 5. Thus, fractions 4 and 5 contained >95% of the (BSA-containing) medium, and <5% of the vesicles. In the final analysis, the relative amount of each sphingolipid present in fractions 4 and 5 ("relative accessibility") was calculated as a percentage of the total amount present in fractions 1–5.

Glucose-6-Phosphatase Latency. As a measure of the intactness of the ER, the latency of glucose-6-phosphatase, an integral membrane protein with its active center in the lumen of the ER, was determined as described (2). The assay is based on the use of an enzyme substrate, mannose-6-phosphate (M6P) which cannot enter intact ER. In short, membranes were isolated at the interface between 1.5 M and 0.6 M sucrose in 10 mM Hepes-NaOH, pH 7.4 (SW60, 30 min, 50,000 rpm, 4°C). Intact and detergent-disrupted membranes (0.1% Triton X-100, 30 min, 0°C) were incubated for 20 min at 30°C (45 mM Hepes-NaOH, pH 6.5) with or without 1 mM M6P, and the amount of inorganic phosphate (Pi) released from M6P was measured colorimetrically. The latency was calculated as (1 − Pi release from M6P in intact membranes/Pi release from M6P in disrupted membranes) × 100%.

Results

Sphingolipid Galactosylation in HepG2 and MDCK II Cells

HepG2 and MDCK II cells were incubated with short-chain NFA- and HFA-ceramide analogs (Table I). The sphingolipid products were identified based on their colocalization with NBD-lipid standards on TLC plates, and their identity was confirmed by α- and/or β-galactosidase digestion, and, in the case of sulfatide, by [^{35}S]sulfation experiments (58). In addition, experiments on isolated membranes showed that the glycosphingolipids only formed if the appropriate nucleotide sugar or sulfate donor was added (not shown). Based on the short-chain sphingolipids that were formed in HepG2 and MDCK II cells (Table I), we decided to use the NFA-ceramide analogue (NBD-Cer) and HepG2 cells to study the galactosyltransferases synthesizing NFA-GalCer and LacCer. MDCK cells and HFA-ceramide were used to characterize the galactosyltransferases responsible for HFA-GalCer and Ga_2Cer.

The use of MDCK cells also allowed us to examine whether NFA- and HFA-GalCer are synthesized by the same or by different galactosyltransferases. This question was addressed by comparing the influence of an inhibitor of sphingolipid synthesis, PDMP (27), on GalCer synthesis from NFA- or HFA-ceramide (Fig. 1). PDMP efficiently inhibited GlcT activity while having little effect on SM-synthase activity. The influence of PDMP on GalCer synthesis depended on the ceramide used. NFA-GalCer synthesis was inhibited by PDMP but to a much lesser extent than synthesis of GlcCer (*A*). This result was confirmed in experiments using short-chain [^{14}C]-Cer instead of NBD-Cer as the NFA-ceramide precursor (not shown). In contrast, the synthesis of HFA-GalCer was not inhibited by the PDMP pretreatment (*B*). These data confirm that PDMP is a rather specific inhibitor of GlcCer synthesis (27), and suggest (but do not prove; see Discussion) the existence of two GalT-1's, one using NFA-ceramide and the other using HFA-ceramide as a substrate.

Table I. Short-Chain Sphingolipid Synthesis in HepG2 and MDCK II Cells

			HepG2		MDCK II	
Enzyme activity	Precursor	Product	NFA	HFA	NFA	HFA
SM-synthase	Cer	SM	+	+	+	+
GlcT	Cer	GlcCer	+	+	+	+
GalT-1	Cer	GalCer	+	−	+	+
GalT-2	ClcCer	LacCer	+	−	−	−
GalT-2b	GalCer	Ga_2Cer	−	−	−	+
GST	GalCer	SGalCer	−	−	−	+

Intact HepG2 and MDCK II cells were incubated with short-chain NFA-Cer (NBD-Cer) or HFA-[^{3}H]-Cer at 37°C, and the sphingolipid products were analyzed as described in Materials and Methods (−, not detected). *GlcT*, glucosyltransferase; *GalT*, galactosyltransferase; *GST*, GalCer sulfotransferase.

Subcellular Distribution of Sphingolipid Galactosylation

Most sphingolipid-synthesizing enzymes colocalized at the Golgi location of the sucrose gradient (Fig. 2). The presence of these enzymes in the Golgi complex of HepG2 cells was confirmed by the effects of BFA. BFA induces relocation of constituents of the Golgi, with the exception of the TGN, to the ER; Golgi relocation is observed in a number of cell lines, including HepG2 (but not in MDCK II; 30, 53). Earlier experiments demonstrated that ~70% of the activity of the Golgi marker enzymes, protein galactosyltransferase and protein sialyltransferase, and 70% of the activity of the sphingolipid glucosyltransferase (GlcT), shifted to the ER recovered in fractions 3–5 of the sucrose gradient (53). Using the same gradient, Fig. 2 confirms

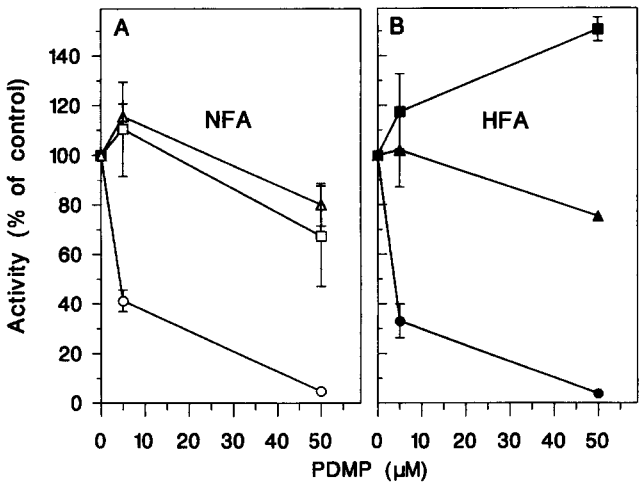

Figure 1. Inhibition of GalCer synthesis by PDMP in MDCK II cells depends on the nature of the ceramide backbone. MDCK II cells were preincubated with PDMP, and the activity of SM-synthase (-△-, -▲-), GalT-1 (-□-, -■-), and GlcT (-○-, -●-) was determined at 37°C using NBD-Cer (*NFA*; *A*), or HFA-[^{3}H]-Cer (*HFA*; *B*). $n = 2$ with a range smaller than symbol size (unless indicated otherwise). 100% corresponds to 460 pmol NFA-SM, 1.5 pmol NFA-GalCer, 130 pmol NFA-GlcCer (*A*), and 1.4 pmol HFA-SM, 10 pmol HFA-GalCer, and 1.7 pmol HFA-GlcCer (*B*). The amount of NBD-GalCer formed was close to background, but the results in *A* were confirmed in an independent experiment using 6-cm instead of 3-cm culture dishes (not shown).

Published April 1, 1996

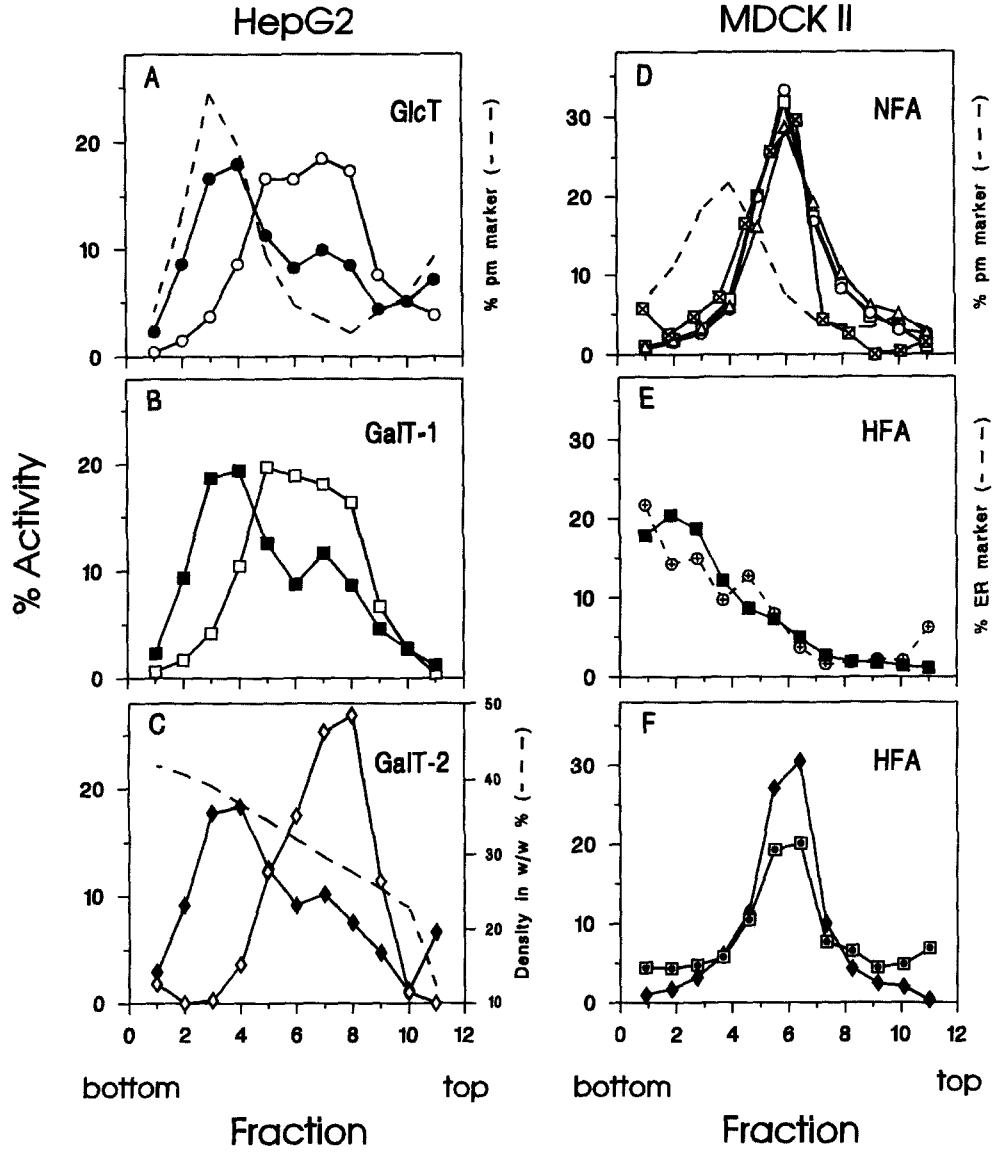

Figure 2. Subcellular distribution of glycosphingolipid synthesizing enzymes in HepG2 and MDCK II. A PNS was subfractionated on 0.7–1.5 M linear sucrose gradients (density profile, *dashed line* in *C*). In *A–C*, HepG2 cells were preincubated in the absence (*open symbols*) or presence (*closed symbols*) of BFA, and subfractions were analyzed for GlcT activity (*A*), GalT-1 activity (*B*), and GalT-2 activity (*C*). In *D–F*, subfractions of MDCK II cells were analyzed, in *D* using NBD-Cer or [^{14}C]-Cer (NFA): SM-synthase (NBD, –△–), NFA-GalT-1 (NBD, –□–; [^{14}C], –⊠–), and GlcT (NBD, –○–); in *E*, using HFA-[^{3}H]-Cer: HFA-GalT-1 (–■–); and in *F*, using HFA-[^{3}H]-GalCer: GalT-2b (–◆–), GST –◙–). The position of the ER was determined by Western blotting with an antibody against calnexin (⊕ in *E*). N-Rh-PE was used as a plasma membrane marker (*dashed line* in *A* and *D*). Enzyme profiles were determined in at least two independent experiments with identical results; the curves represent typical experiments.

these results with respect to GlcT (*A*), and similar effects of BFA were seen on GalT-1 (*B*) and GalT-2 (*C*), supporting their presence in the Golgi complex.

The presence of GlcT, GalT-2b, and GST in the Golgi complex of MDCK II cells was supported by their colocalization with SM-synthase (*D* and *F*), an enzyme which is largely confined to the Golgi complex of MDCK II cells (62). The activity profiles of GlcT and SM-synthase were independent of the precursor used, an NFA-ceramide (*D*), or HFA-ceramide analogue (not shown). NFA-GalT-1 also peaked at the Golgi density, and the same result was obtained when instead of NBD-Cer, radiolabeled short-chain NFA-ceramide was used (*D*). In contrast, HFA-GalT-1 activity peaked near the bottom of the gradient and colocalized with calnexin (*E*), an established ER marker (22). The same result was obtained when HFA-GalT-1 was assayed in the presence of 8 mM CHAPS, or when an excess of nonradioactive short-chain HFA-Cer was included in the assay mixture (not shown). Finally, experiments on intact MDCK II cells demonstrated that short-chain HFA-GalCer is not synthesized at the cell surface (58). These data indicate that the sphingolipid synthesizing enzymes in HepG2 and MDCK II cells are mainly present in the Golgi complex, except HFA-GalT-1, which appears to localize to the ER of MDCK II cells.

Topology of Sphingolipid Galactosylation in HepG2 Cells

The topology of NFA-GalT-1 and GalT-2 was determined by three approaches using NFA-Cer: (*a*) the sidedness of newly synthesized short-chain sphingolipids was determined; (*b*) the sensitivity of the galactosyltransferases towards pretreatment of intact membranes with protease was examined, and (*c*) the galactosyltransferase activities were measured after interfering with the import of UDP-Gal into the Golgi.

Sidedness of Short-Chain Products. As soon as ceramide receives a hydrophilic headgroup, it loses the ability to spontaneously traverse lipid bilayers. The topology of the newly synthesized short-chain sphingolipids can then be probed after opening the cells by adding an acceptor for

Published April 1, 1996

short-chain lipids, for example, BSA (28, 62). BSA cannot penetrate intact membranes and will only deplete the short-chain sphingolipids present in the cytosolic leaflet of organelles. These principles of the BSA sidedness assay were confirmed in experiments on symmetrical lipid vesicles containing a mixture of short-chain sphingolipids (Table II). At a sufficiently high BSA-to-short-chain lipid molar ratio (1,500 in Table II *a*), BSA depleted most of the short-chain ceramides, but not more than 50% of the ceramide derivatives. Fig. 3 *A* shows the results obtained on HepG2 cells permeabilized with the pore-forming toxin streptolysin-O (1). After allowing NBD-sphingolipid synthesis in the permeabilized cells at 10°C, a temperature at which intracellular membrane traffic is blocked, the buffer was replaced by a medium containing BSA. More than 85% of NBD-GlcCer was recovered in the BSA-containing medium, whereas only 14% of NBD-SM was accessible to BSA, fully confirming earlier results (28). In addition, BSA depleted over 92% of newly synthesized NBD-GalCer. The use of cell homogenates allowed for the simultaneous determination of the sidedness of both NBD-GalCer and NBD-LacCer (Fig. 3 *B*). Most NBD-SM and NBD-LacCer were protected against depletion by BSA, whereas most NBD-GalCer and NBD-GlcCer were depleted by the BSA treatment. The same results were obtained when NBD-sphingolipid synthesis was allowed to occur for 30 min at 37°C instead of 3 h at 10°C (87 ± 6% NBD-LacCer and 22 ± 4% NBD-GalCer resisted depletion by BSA).

Several control experiments were performed to exclude a differential sensitivity of the individual NBD-sphingolipid species to depletion by BSA. First, low concentrations of saponin were used to permeabilize the Golgi and allow entry of BSA into the Golgi (43). In the presence of saponin, depletion of all four NBD-sphingolipid species was essentially complete (Fig. 3 *C*). Second, the four NBD-sphingolipid species were depleted from lipid vesicles with similar efficiencies, even at a low BSA-to-short-chain lipid molar ratio (Table II *b*). Finally, when the sidedness of NBD-lipids was determined using dithionite, a chemical that cannot easily permeate membranes and destroys NBD-fluorescence (37), most NBD-SM and NBD-LacCer were protected against dithionite quenching, whereas the fluorescence of most NBD-GalCer and NBD-GlcCer was destroyed (Fig. 3 *D*). In conclusion, newly synthesized short-chain SM and LacCer are detected in the lumenal leaflet, and newly synthesized GlcCer and GalCer in the cytosolic leaflet of the Golgi of HepG2 cells.

Table II. BSA Depletion of Short-Chain Sphingolipids in Symmetrical Lipid Vesicles

		Relative accessibility %							
	BSA/short-chain lipid molar ratio	C6-NBD-					C6-HFA-[^{3}H]-		
		SM	LacCer	GalCer	GlcCer	Cer	GalCer	GlcCer	Cer
(*a*)	0				2	3	2	1	2
	80				29	22	40	40	31
	1500				45	83	50	49	86
(*b*)	80	30	29	24	25				

Large unilamellar vesicles prepared from egg-PC, a nonexchangeable marker (N-Rh-PE), and a mixture of short-chain sphingolipids (total of 1 mol%) were incubated with various concentrations of BSA for 30 min at 20°C. The vesicles were separated from the (BSA-containing) medium by flotation in a sucrose step-gradient, and the relative amount of each sphingolipid species present in the medium was determined (flotation efficiency > 95%; see Materials and Methods). In *a*, vesicles contained 0.3 mol% NBD-GlcCer, NBD-Cer, HFA-[^{3}H]-Cer, 0.01 mol% HFA-[^{3}H]-GalCer, and 0.001 mol% HFA-[^{3}H]-GlcCer, in *b*, 0.2 mol% NBD-SM, NBD-LacCer, NBD-GalCer, and NBD-GlcCer. When the latter vesicles were incubated at a BSA-to-short-chain lipid molar ratio of 800, 43–44% of the short-chain lipids was accessible to BSA.

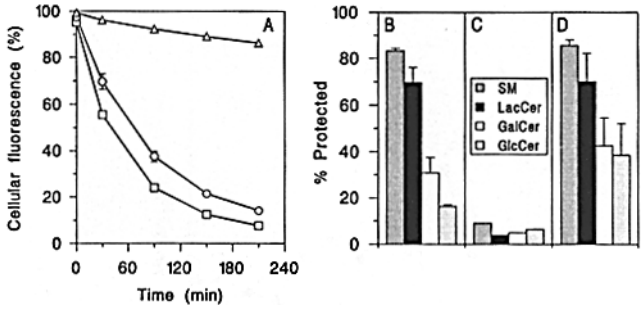

Figure 3. Sidedness of short-chain sphingolipids in permeabilized HepG2 cells and cell homogenates. In *A*, HepG2 cells were permeabilized with SLO, and incubated for 3 h at 10°C with NBD-Cer and UDP-Glc or UDP-Gal. Subsequently, at $t = 0$, BSA was added and the change in cell-associated NBD-fluorescence was followed in time: SM (–△–), GalCer (–□–), and GlcCer (–○–); 100% corresponds to 170 pmol SM ($n = 4$), 9 pmol GalCer ($n = 2$), and 80 pmol GlcCer ($n = 4$). In a parallel experiment on intact cells, BSA depleted 11% of NBD-SM and 14% of NBD-GlcCer (average with $n = 2$; the amount of NBD-GalCer was below the detection limit). In *B–D*, HepG2 cell homogenates were incubated with NBD-Cer at 10°C, and the sidedness of NBD-sphingolipids was assayed, by adding BSA in the absence (*B*; $n = 2$) or presence of 0.1% saponin (*C*), or by selective destruction of NBD fluorescence using dithionite (*D*; $n = 4$). The relative fluorescence protected against BSA back-exchange or dithionite quenching is shown; 100% corresponds to 720 pmol SM, 1.5 pmol LacCer, 8 pmol GalCer, and 1030 pmol GlcCer. Deviations (range or σ_{n-1}) smaller than symbol size (unless indicated otherwise); BSA/NBD-lipid molar ratio of 50 (*B* and *C*).

Protease Sensitivity. The sidedness of the enzymes can also be tested by determining their sensitivity to externally added proteases. Crude Golgi membranes were incubated with pronase E, and the effects on NBD-sphingolipid synthesizing activity were followed in time (Fig. 4 *A*). In agreement with earlier results (28), SM-synthase activity was not inhibited while GlcT activity was quickly impaired. Sphingolipid galactosyltransferase activities were differentially affected by the protease: GalT-1 activity was quickly and almost completely depressed whereas GalT-2 activity was not inhibited. These results suggest that the active centers of NFA-GalT-1 and GalT-2 are located on opposite sides of the Golgi membrane, facing the cytosol and the Golgi lumen, respectively.

Requirement for UDP-Gal Import. Cytosolic UDP-Gal is imported into the Golgi by a specific antiporter (25). Although both NFA-GalT-1 and GalT-2 require UDP-Gal for their activity, only LacCer synthesis should be affected by drugs that reduce UDP-Gal import into the Golgi. The fungal toxin tunicamycin has been shown to inhibit UDP-Gal import into the Golgi, reducing ganglioside GM_1 synthesis from GM_2 without affecting the activity of the responsible galactosyltransferase (65). As expected, tunicamycin strongly inhibited synthesis of NBD-LacCer, while NBD-GlcCer and NBD-GalCer synthesis were not

Published April 1, 1996

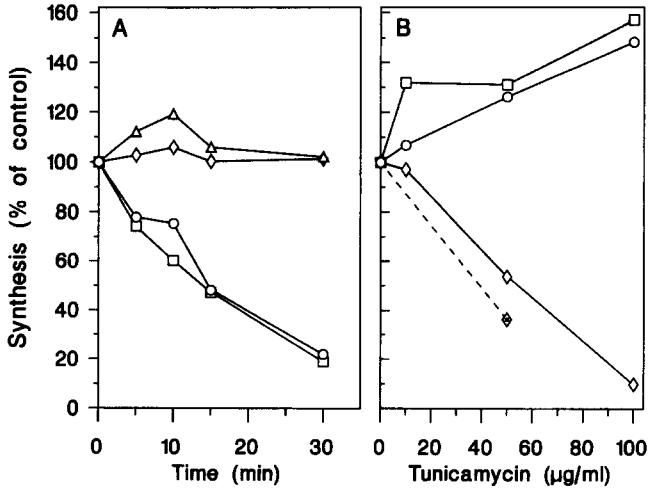

Figure 4. The effects of protease pretreatment and tunicamycin on sphingolipid biosynthesis in the Golgi of HepG2 cells. In *A*, a Golgi membrane fraction was incubated with pronase E at 37°C for the indicated time intervals. The membranes were reisolated and incubated with NBD-Cer to monitor SM-synthase (–△–), GlcT (–○–), and GalT-1 (–□–), and with NBD-GlcCer to monitor GalT-2 (–◇–). In *B*, a PNS was incubated at 37°C with NBD-Cer (*solid lines*) or NBD-GlcCer (*dashed line*) in the presence of tunicamycin; GalT-1 (–□–), GlcT (–○–), and GalT-2 (–◇–, –◈–). The curves represent a typical experiment; 100% corresponds to 50 pmol SM, 3 pmol LacCer, 7 pmol GalCer, and 50 pmol GlcCer (*A*), and 9 pmol LacCer, 1.1 pmol GalCer, and 300 pmol GlcCer (*B*).

inhibited (Fig. 4 *B*). The observed increase in NBD-GlcCer and -GalCer synthesis is probably an indirect effect of a reduction of SM synthesis by tunicamycin (20% reduction at 50 μg/ml). The opposite effects of tunicamycin on GalCer and LacCer synthesis suggest that, in contrast to LacCer synthesis, GalCer synthesis does not depend on UDP-Gal import into the Golgi lumen.

NBD-sphingolipid synthesis was also studied in the CHO mutants Lec8, deficient in UDP-Gal import into the Golgi (16), and Lec2 with normal UDP-Gal import but deficient CMP-sialic acid import (17). These cells contain wild-type levels of galactosyl- and sialyltransferase activities (12, 16, 17). The cell lines synthesized comparable amounts of NBD-SM and NBD-GlcCer (Table III). Lec8 synthesized only slightly less NBD-GalCer than Lec2, but no NBD-LacCer could be detected. This result was confirmed in experiments using NBD-GlcCer instead of NBD-Cer as the precursor (not shown). These data confirm that UDP-Gal import into the Golgi is not required for GalCer synthesis.

Topology of Sphingolipid Galactosylation in MDCK II Cells

MDCK II cells and both NFA- and HFA-ceramide analogues were used to determine the topology of the galactosyltransferases NFA-GalT-1 and GalT-2b in the Golgi, and HFA-GalT-1 in the ER, using the three approaches described for HepG2 cells.

Sidedness of Short-Chain Products. The sidedness of newly synthesized HFA-SM, HFA-GalCer, and HFA-GlcCer in

Table III. Sphingolipid Galactosylation in CHO Lec2 and Lec8 Cell Homogenates

	NBD-lipid synthesis in pmol (and as percent of total)			
Cell line	SM	LacCer	GalCer	GlcCer
Lec2	278.8 (32.2)	9.1 (1.05)	2.1 (0.24)	574.6 (66.5)
Lec8	211.9 (31.5)	ND	1.3 (0.19)	458.7 (68.3)

A PNS (1.6 mg protein/ml) of CHO mutants Lec2 and Lec8 was incubated with NBD-Cer, UDP-Glc, and UDP-Gal for 30 min at 37°C. NBD lipids were quantified as described under Materials and Methods; *ND* (not detected) indicates fluorescence <0.5 pmol.

MDCK II cell homogenates (Table IV) was nearly identical to that of the corresponding NFA-lipids in HepG2 cell homogenates (Fig. 3) and in MDCK II cell homogenates (not shown). SM and Ga_2Cer were largely protected against depletion by BSA, while GalCer and GlcCer were almost completely depleted. Similar results were obtained using a sucrose-Hepes (0.25 M sucrose, 1 mM EDTA, 10 mM Hepes-NaOH, pH 7.4) instead of glutamate-Hepes homogenization buffer (results not shown), and when HFA-sphingolipid synthesis was allowed to occur for 30 min at 37°C instead of 3 h at 10°C (cf. *a* and *b* in Table IV). Control experiments were performed to determine the efficiency with which the short-chain HFA-sphingolipids are depleted by BSA: after intracellular synthesis and transport to the cell surface of intact MDCK II cells at 37°C, all lipid species were removed from the cell surface by BSA with the same efficiency (58). In addition, experiments on lipid vesicles showed that short-chain HFA-sphingolipids and NBD-sphingolipids were depleted by BSA with a similar efficiency (Table II *a*). To exclude the possibility that in a cell homogenate a nonphysiological GalT-1 activity at the cytosolic leaflet of the Golgi or ER is boosted by the excess of UDP-Gal added to the system, intact cells were incubated with HFA-ceramide at 10°C to allow GalCer synthesis under more physiological concentrations of UDP-Gal. After 3 h, the cells were homogenized and the sidedness of the short-chain products was determined (Table IV *c*). Again, the bulk of HFA-GalCer and HFA-GlcCer was accessible to BSA while most of HFA-SM was protected. To extend the results obtained on dog kidney MDCK II cells to the tissue that in vivo expresses the highest levels of GalCer, the sidedness of short-chain HFA-GalCer was determined in the rat Schwann cell line, D6P2T (5). The

Table IV. Sidedness of Short-Chain HFA-Sphingolipids in MDCK II and D6P2T Cell Homogenates

	Protected against BSA as percent of total (pmol synthesized)			
Synthesis conditions	SM	Ga_2Cer	GalCer	GlcCer
(*a*) MDCK II, PNS, 10°C	67 (1.3)	73 (0.03)	14 (1.2)	9 (3.0
(*b*) MDCK II, PNS, 37°C	74 (1.3)	88 (0.25)	30 (4.6)	20 (2.1)
(*c*) MDCK II, intact, 10°C	73 (2.1)	–	31 (2.9)	30 (1.2)
(*d*) D6P2T, PNS, 10°C	57 (0.9)	–	11 (0.7)	3 (2.6)

A PNS of MDCK II cells was incubated with HFA-[^{3}H]-Cer at 10°C (*a*), or, in a parallel experiment, at 37°C (*b*). In *c*, HFA-[^{3}H]-Cer was added to intact MDCK II cells and after 3 h at 10°C, a PNS was prepared. In *d*, a PNS of D6P2T cells was incubated with HFA-[^{3}H]-Cer as in *a*. The sidedness of HFA-sphingolipids was determined using the BSA assay as described in Materials and Methods. The amount of Ga_2Cer formed at 10°C in intact cells and in D6P2T cell homogenates was below the detection limit. The BSA-to-short-chain lipid molar ratios were >18,000.

Published April 1, 1996

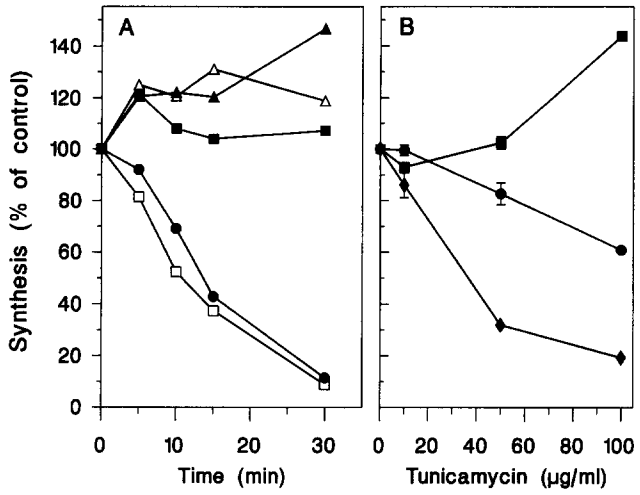

Figure 5. The effects of protease pretreatment and tunicamycin on sphingolipid biosynthesis in the Golgi and ER of MDCK II cells. After pronase treatment and reisolation of the membranes (*A*), enzyme activities were assayed with NBD-Cer (*open symbols*) or with HFA-[^{3}H]-Cer (*closed symbols*): SM-synthase (–△–, –▲–), GalT-1 (–□–, –■–), and GlcT (–●–; same result using NBD-Cer, not shown). The curves represent typical experiments. In *B*, a PNS was incubated at 37°C in the presence of tunicamycin with HFA-[^{3}H]-Cer to determine the activity of HFA-GalT-1 (–■–), GlcT (–●–), and GalT-2b (–◆–). 100% values correspond to 120 pmol NFA-SM, 10 pmol NFA-GalCer, 8 pmol HFA-SM, 3 pmol HFA-GalCer, and 30 pmol HFA-GlcCer (*A*), and 50 pmol HFA-GalCer, 130 pmol HFA-GlcCer, and 7 pmol HFA-Ga_2Cer (*B*; $n = 2$ with range smaller than symbol size, unless indicated otherwise). The results of *A* and *B* were confirmed using HFA-[^{3}H]-Cer in the presence of a 30-fold excess of nonradioactive HFA-Cer (not shown).

results (Table IV *d*) were very similar to the results obtained on MDCK II cells (Table IV *a*). In conclusion, newly synthesized short-chain HFA-GalCer is present at the cytosolic surface of the ER, and short-chain NFA-GalCer at the cytosolic surface of the Golgi. In contrast, newly synthesized short-chain Ga_2Cer remains confined to the luminal leaflet of the Golgi.

Protease Sensitivity. In agreement with the results obtained on HepG2 (Fig. 4 *A*), SM-synthase activity was not inhibited by the pronase treatment while GlcT and NFA-GalT-1 activity were quickly reduced (Fig. 5 *A*). Pronase treatment did not inhibit HFA-GalT-1 activity, and the same result was obtained if trypsin instead of pronase was used (not shown). By omitting the membrane pelleting step after protease treatment, the effects of detergent addition on the protease sensitivity of HFA-GalT-1 could be studied. HFA-GalT-1 activity was extremely protease resistant in intact membranes, but became protease sensitive after membrane solubilization (Table V). These data strongly suggest that HFA-GalT-1 has its active center in the lumen of the ER.

Requirement for UDP-Gal Import. The effects of tunicamycin on HFA-sphingolipid synthesis were examined (Fig. 5 *B*). The synthesis of HFA-GalCer and NFA-GalCer (not shown) were not inhibited, whereas synthesis of HFA-Ga_2Cer was clearly inhibited. With respect to NFA-GalCer and HFA-Ga_2Cer, these results are in line with the results

Table V. HFA-GalT-1 Becomes Protease Sensitive after Membrane Solubilization

	Protease to membrane protein ratio	Residual HFA-lipid synthesis activity (percent of untreated control)	
Detergent	(wt:wt)	GalCer	GlcCer
None	1:5	116:8	3.9
None	1:1	85.5	0.4
TX-100 (0.1%)	1:5	14.4	–
TX-100 (0.1%)	1:1	8.4	–
CHAPS (8 mM)	1:5	64.4	5.1
CHAPS (8 mM)	1:1	26.1	1.1

A Golgi-ER membrane fraction from MDCK II cells was preincubated with pronase E, in the absence or presence of detergent. Membranes were not reisolated but immediately incubated with HFA-[^{3}H]-Cer and nucleotide sugars at 37°C. The residual HFA-lipid synthesis activity is shown as a percentage of the HFA-lipid synthesis activity in a control sample not treated with pronase. In the untreated controls and in the absence of detergent, 100% values corresponded to 2.8 pmol HFA-GalCer and 8.0 pmol HFA-GlcCer. The addition of Triton or CHAPS changed these values to 2.6 and 1.2% for HFA-GalCer, and to 0.1 and 10.2% for HFA-GlcCer, respectively. The GlcCer signal in the presence of Triton was too low to allow reliable quantitation of the effect of protease treatment.

obtained on BSA accessibility and protease sensitivity (Table IV and Fig. 5 *A*), suggesting that NFA-GalCer and HFA-Ga_2Cer synthesis occur in the cytosolic and lumenal leaflet of the Golgi, respectively. The fact that HFA-GalCer synthesis was not inhibited by tunicamycin suggests that the availability of UDP-Gal in the ER lumen is not affected by tunicamycin (see Discussion).

Transbilayer Movement of Monohexosyl Sphingolipids in ER and Golgi

If HFA-GalT-1 is active in the lumen of the ER, HFA-GalCer can only become accessible to BSA after translocating from the lumenal to the cytosolic leaflet of the ER. Because such a translocation event is expected to be both time- and temperature-dependent (24, 57), a PNS of MDCK II cells was incubated with HFA-ceramide for only 30 min at 0°C. BSA was added, and the accessibility of HFA-GalCer to BSA was followed in time at 10°C (Fig. 6). As before (Table IV), most HFA-SM and hardly any HFA-GlcCer was protected against BSA. However, almost 50% of HFA-GalCer was protected against BSA at the earliest time point ($t = 5$ min), and only became accessible after a prolonged incubation. As argued before, the capacity of BSA to deplete short-chain lipids is very similar for all ceramide derivatives tested. In experiments on lipid vesicles, the efficiency with which BSA depleted HFA-GalCer and -GlcCer was found to be identical, even at a low BSA-to-short-chain lipid molar ratio (Table II *a*).

Moreover, the luminal ER enzyme glucose-6-phosphatase remained >93% latent during the BSA incubation (Fig. 6), suggesting that the release of HFA-GalCer from the ER was not due to a deterioration of the ER membrane. Thus, the difference in the percentage of HFA-GalCer and the percentage of HFA-GlcCer depleted by BSA suggests that HFA-GalCer is synthesized in the lumenal leaflet of the ER and translocates to the cytosolic surface of the ER before it is depleted by BSA, whereas HFA-GlcCer is synthesized in the cytosolic leaflet (of the Golgi) and is, therefore, immediately accessible to BSA.

Published April 1, 1996

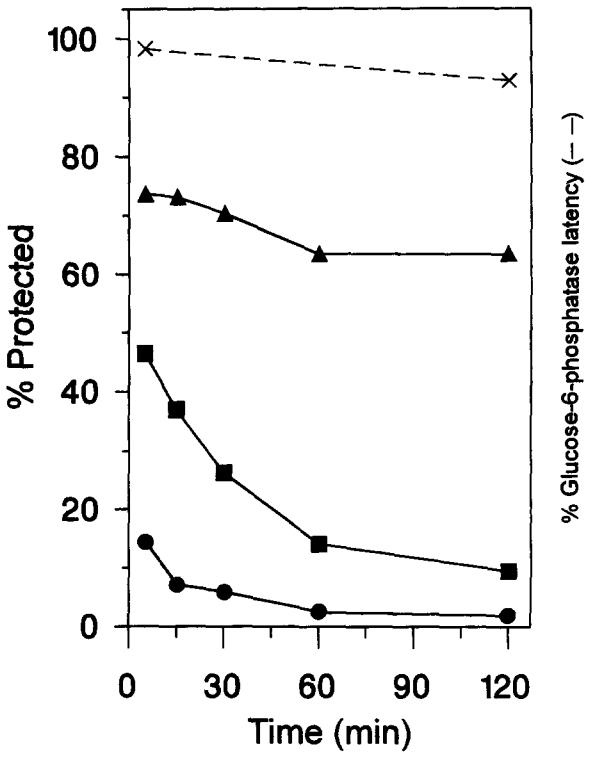

Figure 6. The accessibility of short-chain HFA-GalCer to BSA in MDCK II cell homogenates increases during a BSA incubation. A PNS was incubated with HFA-[^{3}H]-Cer for 30 min at 0°C, and the sidedness of newly synthesized HFA-sphingolipids was determined after an incubation with BSA at 10°C for the indicated time intervals (see Materials and Methods). HFA-SM (-▲-), HFA-GalCer (-■-), and HFA-GlcCer (-●-). The results of a typical experiment are shown; 100% values at t = 5 min (60 min) correspond to 0.31 (0.26) pmol HFA-SM, 0.12 (0.14) pmol HFA-GalCer, and 0.14 (0.20) pmol HFA-GlcCer. BSA/HFA-lipid molar ratio of 18,000. In an independent experiment, the intactness of the ER was checked by determining the latency of the lumenal ER enzyme, glucose-6-phosphatase (*dashed line*; average, n = 2).

The data presented so far clearly indicate that in analogy to LacCer, Ga_2Cer is synthesized in the luminal leaflet of the Golgi, whereas their direct precursors, with the exception of HFA-GalCer, are synthesized in the cytosolic leaflet of the Golgi. To follow the transbilayer movement of GalCer, cell homogenates were incubated with GalCer, the synthesis of higher products was monitored, and their sidedness was determined (Table VI). Because the amount of higher products that formed turned out to be highly temperature-sensitive, experiments were carried out at 37°C. By adding PAPS to an MDCK II cell homogenate, SGalCer synthesis could now be monitored. In Table VI *a*, an MDCK II cell homogenate was incubated with HFA-[^{3}H]-Cer: Ga_2Cer and SGalCer were formed, and in both cases >80% was protected against BSA. Direct evidence for the translocation of HFA-GalCer to the lumenal leaflet of the Golgi membrane was obtained by using HFA-GalCer as the precursor: Ga_2Cer and SGalCer formed and both were largely protected against BSA back-exchange (Table VI *b*). Essentially the same result was obtained when NBD-GalCer was used as the precursor (Table VI *c*). Convincing evidence for the translocation of GlcCer to the lumenal leaflet of the Golgi of HepG2 cells was also obtained (Table VI, *d* and *e*). Thus, not only short-chain analogues of GlcCer, but also short-chain analogues of NFA- and HFA-GalCer are able to translocate from the cytosolic to the luminal leaflet of the Golgi, where they are used for higher glycosphingolipid synthesis.

Discussion

We used short-chain NFA- and HFA-ceramide analogues to determine the intracellular localization and the topology of early sphingolipid galactosylation. The use of NFA-ceramide analogues and HepG2 cells offered the opportunity to directly compare the topology of NFA-GalT-1 and GalT-2, while NFA- and HFA-ceramide analogues and MDCK II cells allowed a comparison between NFA-GalT-1, HFA-GalT-1, GalT-2b, and GST (see Table I).

NFA-GalT-1 and GalT-2 Have an Opposite Topology

Earlier subfractionation experiments indicated that GlcT and GalT-2 are present in the Golgi complex (20, 28, 56), and the effects of BFA on the subcellular distribution of GlcT and GalT-2 in HepG2 cells (Fig. 2) led us to the same conclusion. Moreover, like GlcT and GalT-2, the NFA-GalT-1 activity in HepG2 cells could be assigned to the proximal part of the Golgi complex. With respect to the topology of GalT-2, our data confirmed the results obtained by Lannert et al. (33) and lead to the conclusion that the active center of GalT-2 is located in the lumen of the Golgi.

An opposite conclusion was reached by Trinchera et al. (55), mainly based on a comparison of intact and detergent-permeabilized Golgi, and the assumption that Golgi permeabilization should boost the activity of lumenal enzymes by increasing their substrate supply. An increase in the activity of GalT-2 was not observed, and the authors concluded that GalT-2 is active at the cytosolic surface of the Golgi. However, in these types of experiments reliable conclusions on enzyme topology can only be drawn if direct effects of detergent addition on enzyme activity are excluded. In our hands, (NBD-)LacCer synthesis is strongly inhibited by detergent addition (unpublished observation). The finding that Sepharose-immobilized GlcCer can be used by GalT-2 present in an "intact" Golgi preparation (55) may be explained by the presence of inside-out or leaky Golgi cisternae; an asialofetuin-SAT latency of 81–84% (55) indicates that 16–19% of the Golgi vesicles must have been inside-out or leaky.

In contrast to GalT-2, NFA-GalT-1 is active at the cytosolic surface of the Golgi complex: NBD-GalCer was accessible to BSA, and NFA-GalT-1 activity was rapidly impaired by pronase treatment, the enzyme activity was not reduced by tunicamycin, and NBD-GalCer synthesis was quite normal in CHO Lec8 cells known to be deficient in UDP-Gal import into the Golgi (Figs. 2–4, Table III). After synthesis in the Golgi complex, NBD-GalCer efficiently reached the cell surface of intact HepG2 cells at 37°C (Burger, K.N.J., unpublished observations). This implies that at some stage during or after transport to the plasma membrane, GalCer, like GlcCer, undergoes transbilayer movement.

Published April 1, 1996

Table VI. Short-Chain Analogues of GalCer and GlcCer Are Used for Higher Glycosphingolipid Synthesis in the Lumen of the Golgi

Incubation conditions		Percent protected against BSA (pmol synthesized)					
Cell line	Precursor	SM	Ga_2Cer	SGalCer	GalCer	GlcCer	LacCer
(*a*) MDCK II	HFA-[^{3}H]-Cer	82 (3.9)	90 (1.9)	81 (1.4)	37 (14.4)	35 (2.9)	
(*b*) MDCK II	HFA-GalCer		85 (1.9)	79 (1.6)			
(*c*) MDCK II	NBD-GalCer		70 (46.0)	84 (10.6)			
(*d*) HepG2	NBD-GlcCer						88 (47.0)
(*e*) HepG2	NBD-GlcCer						7 (47.0)

A PNS of MDCK II cells was incubated for 30 min at 37°C with UDP-Gal, PAPS, and HFA-[^{3}H]-Cer (*a*), HFA-GalCer (*b*), or NBD-GalCer (*c*) and the sidedness of newly synthesized sphingolipids was determined. In a similar experiment, a PNS of HepG2 cells was incubated at 37°C with UDP-Gal and NBD-GlcCer, and the sidedness of the sphingolipids was determined in the absence (*d*) or presence (*e*) of 0.1% saponin. The results of a typical experiment are shown. Sidedness determined using BSA; BSA-to-short-chain lipid molar ratios >20,000 (in *a* and *b*) and 700 (in *c*, *d*, and *e*).

Two Different Ceramide Galactosyltransferase Activities in MDCK II Cells

While HepG2 cells contain only trace amounts of GalCer (50), MDCK II cells contain substantial amounts of GalCer and higher derivatives (11, 23, 39). In subfractionation experiments (Fig. 2), NFA-GalT-1, GalT-2b, and GST colocalized at the Golgi location of the sucrose gradient. In contrast, HFA-GalT-1 activity was found at a higher density of the gradient, colocalizing with an ER marker. Recently, a GalT-1 was cloned from rat brain (47, 48, 51), and a number of findings suggests that the HFA-GalT-1 of MDCK II cells is the dog homologue of this cloned GalT-1. First, Northern blot analysis revealed its presence in the nervous system, but also in rat kidney (48, 51). Second, lectin-blotting experiments on GalT-1 purified from rat brain suggest a glycoprotein of the high-mannose type, i.e., a typical ER resident protein (48). In addition, the protein contains an ER retrieval signal KKXX at its COOH terminus (see reference 40). Proteins with this double lysine motif have occasionally been found to localize to the intermediate compartment (for review see reference 40), but this is unlikely for HFA-GalT-1: HFA-GalT-1 colocalizes with an ER marker at high density of the sucrose gradient (Fig. 2), while, in general, enzymes of the intermediate compartment cofractionate with (*trans*)Golgi markers at a lower density (22, 49). Finally, cells transfected with the GalT-1 cDNA have an increased capacity to synthesize GalCer, the enzyme prefers HFA-ceramide as a substrate (38, 47; in contrast to the GlcT, 63), and it localizes to the ER (van der Bijl, P., G.J. Strous, M. Lopes-Cardozo, J. Thomas-Oates, and G. van Meer, manuscript submitted for publication).

The presence of two separate GalT-1 activities is further supported by several findings. First, protease treatment of intact membranes destroyed NFA-GalCer biosynthesis while leaving HFA-GalCer biosynthesis unaffected (Fig. 5). Second, NFA-GalCer biosynthesis was strongly inhibited by the addition of UDP-Glc to the assay system while HFA-GalCer biosynthesis was not affected (Burger, K.N.J., and P. van der Bijl, unpublished observations). Finally, a potent inhibitor of glucosylceramide biosynthesis, PDMP (27), mildly inhibited NFA-GalCer synthesis, but not the synthesis of HFA-GalCer (Fig. 1). In MDCK II cells, HFA-GalCer is clearly not synthesized by the GlcT. However, our data do not completely exclude this possibility for NFA-GalCer: NFA-GalT-1 and GlcT colocalize on a sucrose gradient and share the same topology (see below), and NFA-GalCer synthesis is strongly inhibited in the presence of UDP-Glc. The differential effect of PDMP on the synthesis of GlcCer and NFA-GalCer (Fig. 1 *A*) suggests the presence of a separate galactosyltransferase responsible for the formation of NFA-GalCer, but alternative explanations are possible, for example, UDP-Gal might interfere with the binding of PDMP to GlcT. The question of the identity of NFA-GalT-1 is particularly relevant in myelin-forming cells, oligodendrocytes, and Schwann cells, which produce large amounts of both NFA- and HFA-GalCer, and have a relatively low GlcT activity (19, 46). More research will be required to determine whether in these tissues NFA-GalCer is synthesized by a separate NFA-GalT-1, by the GlcT, or by the HFA-GalT-1.

Topology of GalCer-based Glycosphingolipid Biosynthesis and Transbilayer Movement of GalCer

Our topology studies in MDCK II assign the GalT-2b activity to the Golgi lumen, and, as in HepG2, the NFA-GalT-1 activity to the cytosolic surface of the Golgi (Table IV, Fig. 5). The topology of GST was studied less rigorously, but newly synthesized short-chain SGalCer was found protected against BSA back-exchange, directly supporting the conclusion of Tennekoon et al. (54) that sulfatide is synthesized in the lumenal leaflet of the Golgi membrane. In MDCK II cells, >90% of endogenous Ga_2Cer and SGalCer contains an NFA-ceramide backbone (39). Assuming the NFA-GalT-1 activity detected in vitro is also responsible for the biosynthesis of NFA-GalCer in vivo, our topology results imply that NFA-GalCer must translocate from the cytosolic to the lumenal leaflet of the Golgi membrane in order to become available to GalT-2b and GST. Indeed, when NBD-GalCer was added to intact Golgi membranes, it was converted to NBD-Ga_2Cer and NBD-SGalCer in the lumen of the Golgi (Table VI). Transbilayer movement is also required for NFA-GalCer to reach the cell surface; newly synthesized short-chain NFA-GalCer is transported efficiently to the cell surface of intact MDCK II cells (58).

In contrast to NFA-GalCer, HFA-GalCer is not synthesized in the Golgi complex but in the ER of MDCK II cells. As argued before, the HFA-GalT-1 detected in MDCK II cells is closely related to the GalT-1 cloned from

Published April 1, 1996

rat brain (47, 48, 51). The cDNA sequence predicts a type I glycoprotein of 521 amino acids with its active center in the lumen of the ER. It shows significant homology to mammalian UDP-glucuronyltransferases, which have their active center exposed towards the lumen of the ER in liver and kidney (10, 18). A lumenal orientation of HFA-GalT-1 in the ER of MDCK II cells is supported by our finding that in contrast to NFA-GalCer synthesis, HFA-GalCer synthesis is only inhibited by protease after membrane solubilization (Table V, Fig. 5).

Short-chain HFA-GalCer appears to have access to the cytosolic surface of the ER despite it being synthesized in the lumenal leaflet of the ER (Fig. 6). Though most phospholipids are synthesized in the ER, HFA-GalCer is the only glycosphingolipid so far found to be synthesized in the ER. Phospholipids, including the sphingolipid SM and the glycophospholipid phosphatidylinositol, are able to move quickly across the ER bilayer with a half-time of ~20 min at 37°C; translocation is bidirectional, ATP-independent, protein-mediated, and has a low lipid specificity (4, 7, 24, 66). Future experiments will have to resolve whether HFA-GalCer uses the same "flippase" that moves phospholipids across the ER bilayer.

Because sugar nucleotides are synthesized in the cytosol (13), the presence of the active center of HFA-GalT-1 in the lumen of the ER immediately raises the question how UDP-Gal enters the ER lumen. The ER is able to import UDP-Glc (25, 42), but UDP-Glc cannot support HFA-GalCer synthesis (subfractionation experiment; not shown). So far, only the Golgi has been found to import UDP-Gal; import occurs via an antiport system in which UDP-Gal is exchanged with UMP present in the Golgi lumen (for a review see reference 25). Our finding that the synthesis of HFA-GalCer in the ER is not inhibited by tunicamycin (Fig. 5 *B*) suggests that the mechanism by which UDP-Gal enters the ER differs from that in the Golgi complex. However, it is currently unclear how UDP-Gal enters the ER lumen. On the one hand, UDP-Gal import was shown to be absent in membrane vesicles derived from rat liver ER (42), suggesting that the capacity to import UDP-Gal into the ER may only be present in those specialized cell types that are capable of synthesizing HFA-GalCer. On the other hand, COS and CHO cells transfected with the cloned GalT-1 cDNA efficiently synthesize HFA-GalCer (47; van der Bijl, P., G.J. Strous, M. Lopes-Cardozo, J. Thomas-Oates, and G. van Meer, manuscript submitted for publication) arguing against this possibility.

After translocation to the cytosolic surface of the ER, a second transbilayer movement would be required to make HFA-GalCer available to GalT-2b and GST in the lumen of the Golgi. This possibility of a reverse translocation of HFA-GalCer in the Golgi complex is supported by results showing that when short-chain HFA-GalCer is added to intact Golgi membranes, it is converted to HFA-Ga_2Cer and HFA-SGalCer in the lumen of the Golgi (Table VI). Though there is no obvious reason why short-chain HFA-GalCer would be translocated to the cytosolic surface of the ER more efficiently than endogenous, long-chain, HFA-GalCer (see for example reference 14), additional experiments are required before our results can be extended to the behavior of natural HFA-GalCer. Part of the HFA-GalCer synthesized, in vivo, may not translocate to the cytosolic leaflet of the ER, and reach the lumenal leaflet of the Golgi after vesicular transport. In that case, translocation of HFA-GalCer in the Golgi complex would not be required for higher glycosphingolipid biosynthesis. In contrast, the formation of higher derivatives of NFA-GalCer and GlcCer appears to be absolutely dependent on transbilayer movement in the Golgi complex. For similar reasons, transport of NFA-GalCer and GlcCer to the cell surface depends on transbilayer movement, whereas this may not be required for HFA-GalCer.

Implications for Biosynthesis and Intracellular Transport of Glycosphingolipids

Fig. 7 combines our experimental data with data from literature to illustrate the steps involved in early sphingolipid glycosylation and in the intracellular transport of glycosphingolipids to the cell surface. The three key features are (*1*) exposure of newly synthesized monohexosyl sphingolipids to the cytosol, (*2*) translocation of HFA-GalCer from the lumenal to the cytosolic leaflet of the ER membrane, and (*3*) translocation of monohexosyl sphingolipids from the cytosolic to the lumenal leaflet of the Golgi membrane.

All three monohexosyl sphingolipids are, at least transiently, exposed to the cytosol and may interact with cytosolic proteins. First, the rather unexpected presence of GalCer at the cytosolic surface of the ER and Golgi may allow interaction of these organelles with members of the large family of cytosolic galactose-binding lectins (6). Second, the monohexosyl sphingolipids at the cytosolic surface of ER and Golgi could, in principle, exchange through the cytosol, possibly with the help of transfer proteins and reach other membranes by a nonvesicular transport mechanism. Such a transport mechanism may exist for GlcCer in BFA-treated CHO cells: transport of newly synthesized SM and GM_3 to the plasma membrane was inhibited, but transport of GlcCer was not affected (64). In addition, a glycosphingolipid transfer protein has been described which is capable of transferring both GlcCer and GalCer from donor to target membranes, in vitro (44, 45). However, it is unclear if lipid transfer proteins have a similar function in vivo, and kinetic data suggest that, like SM, most GlcCer is transported to the cell surface by a vesicular mechanism (61). Finally, the presence of GlcCer and GalCer in the cytosolic leaflet of the Golgi complex, implies that these glycosphingolipids may aggregate and form microdomains at the cytosolic surface of the Golgi complex. So far, only aggregation of glycosphingolipids in the lumenal leaflet of the *trans*-Golgi network has been considered.

The second important feature of Fig. 7 is the translocation of a glycosphingolipid, HFA-GalCer, from the luminal to the cytosolic leaflet of the ER membrane (*d* in Fig. 7). Preliminary experiments suggest that, in principle, even glycosphingolipids with a bulkier headgroup than GalCer may be able to move across the ER bilayer: if HepG2 cells are treated with BFA to relocate GalT-2 to the ER (see Fig. 2), a steep increase is observed in the percentage NBD-LacCer accessible to BSA back-exchange (Burger, K.N.J., unpublished data). The low sphingolipid content of the ER indicates that most sphingolipids synthesized in

Published April 1, 1996

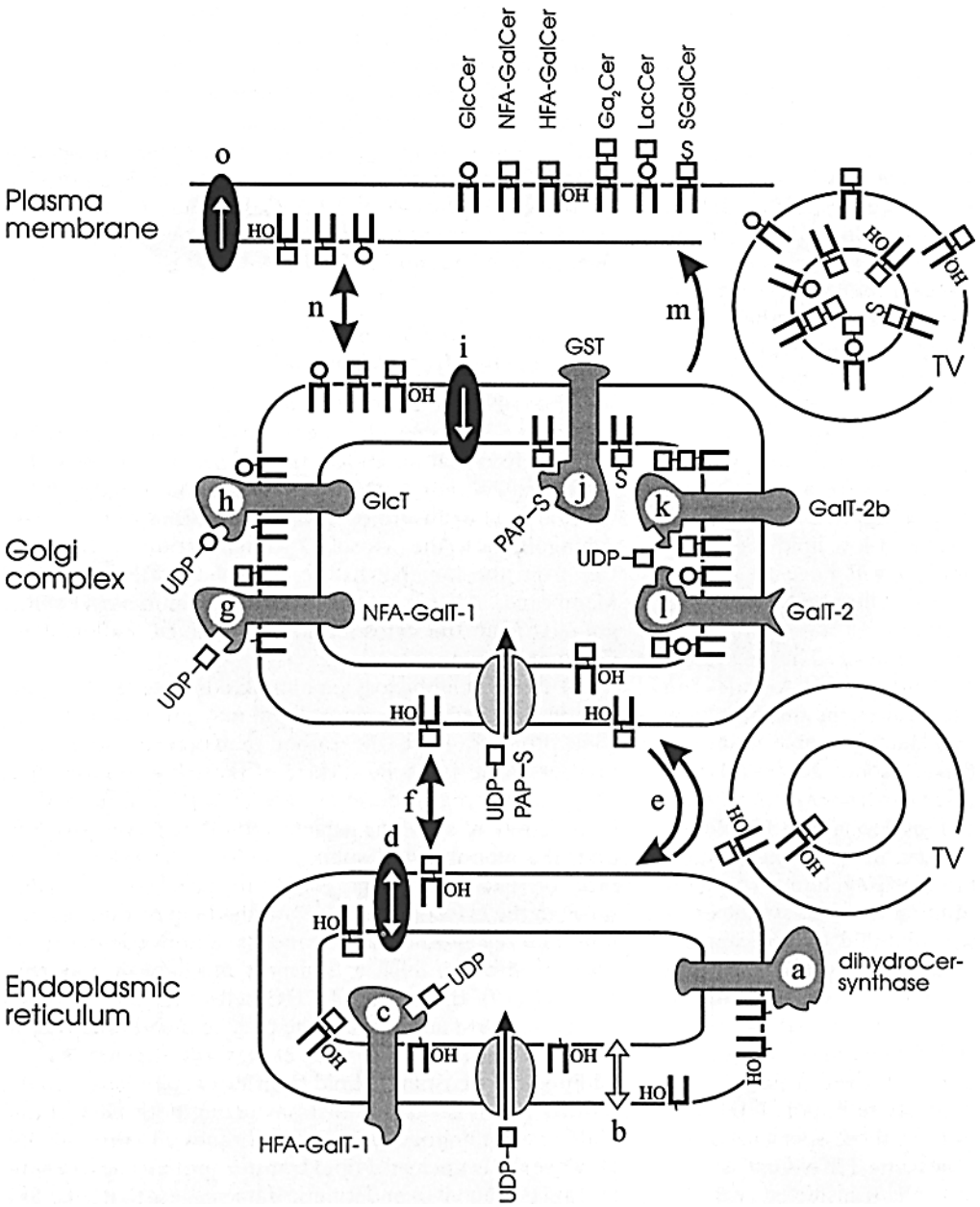

Figure 7. Schematic model for the topology of early sphingolipid glycosylation. The formation of dihydro-Cer (*a*) occurs at the cytosolic surface of the ER (26, 35). Ceramide undergoes rapid spontaneous transbilayer movement (*b*). HFA-Cer is converted into HFA-GalCer in the lumenal leaflet of the ER (*c*), but is able to translocate to the cytosolic leaflet possibly using the bidirectional phospholipid flippase (*d*). HFA-GalCer moves to the Golgi complex in transport vesicles (*e*), or, possibly, via monomeric exchange (*f*). NFA-GalCer and GlcCer are synthesized at the cytosolic face of the Golgi (*g* and *h*). Monohexosyl sphingolipids are able to translocate from the cytosolic to the lumenal leaflet of the Golgi membrane (*i*), and act as substrates for enzymes involved in higher glycosphingolipid synthesis (*j*, *k*, and *l*). Higher glycosphingolipids reach the cell surface in the lumenal leaflet of transport vesicles (*m*). Current evidence indicates this route is also followed by the bulk of monohexosyl sphingolipids. The same translocator in the Golgi (*i*) may be required for both substrate supply to higher glycosphingolipid synthesizing enzymes, and cell surface expression of monohexosyl sphingolipids. Some monohexosyl sphingolipids may reach the cytosolic leaflet of the plasma membrane after vesicular transport or by monomeric exchange through the cytosol (*n*). However, there is currently no evidence supporting the presence of a sphingolipid translocator in the plasma membrane (*o*). Note that the exact intracellular distribution of enzymes can only be revealed using immuno-EM requiring specific antibodies which are not yet available for the sphingolipid synthesizing enzymes shown. The Golgi enzymes are not necessarily present in the same Golgi cisternae, and, in some cell types, part of the enzyme activities may also be present outside the ER/Golgi, e.g., at the plasma membrane. Of the enzymes shown, only HFA-GalT-1 has been cloned. *Square*, galactose; *circle*, glucose; *TV*, transport vesicle; *S*, sulfate.

the Golgi must be excluded from retrograde transport to the ER. However, in view of the large size of the retrograde transport pathway, it is unlikely that all sphingolipids would be excluded from retrograde traffic. Indeed, Forssman, a globoside synthesized in the Golgi complex, has been detected in the nuclear envelope of MDCK II cells by immunoelectron microscopy (60). Sphingolipids, like Forssman, that do reach the ER, may have access to the cytosolic surface of the ER through the action of the phospholipid flippase. Retrograde traffic and transbilayer movement in the ER might be the mechanism by which "luminal" lipids such as the gangliosides GM_2 and GM_3, and the globoside Gb_4Cer reach the cytosol and bind to the cytoskeleton (21, 32).

The most striking result of our topology study is the ability of all three monohexosyl sphingolipids to translocate from the cytosolic to the luminal leaflet of the Golgi membrane (*i* in Fig. 7). In the translocation assays, we used the conversion of monohexosyl sphingolipids into higher products in the lumenal leaflet of the Golgi as evidence for sphingolipid translocation. Although kinetic data cannot be obtained, these assays already reveal some

important characteristics of monohexosyl sphingolipid translocation in the Golgi. Translocation of GlcCer and GalCer can be uncoupled from their biosynthesis, suggesting that separate proteins are responsible for monohexosyl sphingolipid biosynthesis and translocation. In addition, translocation does not require cytosolic proteins and is most likely not ATP dependent, suggesting that translocation occurs through facilitated transport.

Because the bulk of monohexosyl sphingolipids appears to translocate to the luminal leaflet of the Golgi before arrival at the plasma membrane (61), the same translocator in the Golgi is probably required for both substrate supply to higher glycosphingolipid synthesizing enzymes, and cell surface expression of monohexosyl sphingolipids. Clearly, the identification and characterization of the monohexosyl sphingolipid translocator(s) will be of great importance in understanding how cells regulate the glycosphingolipid composition of their cell surface.

We are grateful to Ardy van Helvoort for blotting, to Ari Helenius (New Haven, CT) for providing anti-calnexin antibodies, to Jan Willem Kok (Groningen, NL) for NBD-LacCer, and to Norman Radin (Ann Arbor, MI) for valuable advice on the use of PDMP. We thank Ger Strous for critically reading the manuscript.

This study was supported by European Community contract BIO2-CT93-0348 (K. Burger and G. van Meer).

Received for publication 8 August 1995 and in revised form 21 December 1995.

References

1. Ahnert-Hilger, G., W. Mach, K.J. Föhr, and M. Gratzl. 1989. Poration by α-toxin and streptolysin O: an approach to analyze intracellular processes. *Methods Cell Biol.* 31:63–90.
2. Arion, W.J. 1989. Measurement of intactness of rat liver endoplasmic reticulum. *Methods Enzymol.* 174:58–67.
3. Babia, T., J.W. Kok, M. van der Haar, R. Kalicharan, and D. Hoekstra. 1994. Transport of biosynthetic sphingolipids from Golgi to plasma membrane in HT29 cells: involvement of different carrier vesicle populations. *Eur. J. Cell Biol.* 63:172–181.
4. Backer, J.M., and E.A. Dawidowicz. 1987. Reconstitution of a phospholipid flippase from rat liver microsomes. *Nature (Lond.).* 327:341–343.
5. Bansal, R., and S.E. Pfeiffer. 1987. Regulated galactolipid synthesis and cell surface expression in Schwann cell line D6P2T. *J. Neurochem.* 49:1902–1911.
6. Barondes, S.H., D.N.W. Cooper, M.A. Gitt, and H. Leffler. 1994. Galectins: structure and function of a large family of animal lectins. *J. Biol. Chem.* 269:20807–20810.
7. Bishop, W.R., and R.M. Bell. 1988. Assembly of phospholipids into cellular membranes: biosynthesis, transmembrane movement and intracellular translocation. *Annu. Rev. Cell Biol.* 4:579–610.
8. Bligh, E.G., and W.J. Dyer. 1959. A rapid method of total lipid extraction and purification. *Can. J. Biochem. Physiol.* 37:911–917.
9. Bonner, W.M., and J.D. Stedman. 1978. Efficient fluorography of ^{3}H and ^{14}C on thin layers. *Anal. Biochem.* 89:247–256.
10. Bossuyt, X., and N. Blanckaert. 1994. Carrier-mediated transport of intact UDP-glucuronic acid into the lumen of endoplasmic-reticulum-derived vesicles from rat liver. *Biochem. J.* 302:261–269.
11. Brändli, A.W., G.C. Hansson, E. Rodriguez-Boulan, and K. Simons. 1988. A polarized epithelial cell mutant deficient in translocation of UDP-galactose into the Golgi complex. *J. Biol. Chem.* 263:16283–16290.
12. Briles, E.B., E. Li, and S. Kornfeld. 1977. Isolation of wheat germ agglutinin-resistant clones of Chinese hamster ovary cells deficient in membrane sialic acid and galactose. *J. Biol. Chem.* 252:1107–1116.
13. Coates, S.W., T. Gurney, W.L. Sommers, N. Yeh, and C.B. Hirschberg. 1980. Subcellular localization of sugar nucleotide synthetases. *J. Biol. Chem.* 255:9225–9229.
14. Connor, J., C.H. Pak, R.F. Zwaal, and A.J. Schroit. 1992. Bidirectional transbilayer movement of phospholipid analogs in human red blood cells. Evidence for an ATP-dependent and protein-mediated process. *J. Biol. Chem.* 267:19412–19417.
15. Coste, H., M.B. Martel, and R. Got. 1986. Topology of glucosylceramide synthesis in Golgi membranes from porcine submaxillary glands. *Biochim. Biophys. Acta.* 858:6–12.
16. Deutscher, S.L., and C.B. Hirschberg. 1986. Mechanism of galactosylation in the Golgi apparatus. A Chinese hamster ovary cell mutant deficient in translocation of UDP-galactose across Golgi vesicle membranes. *J. Biol. Chem.* 261:96–100.
17. Deutscher, S.L., N. Nuwayhid, P. Stanley, E.I.B. Briles, and C.B. Hirschberg. 1984. Translocation across Golgi vesicle membranes: a CHO glycosylation mutant deficient in CMP-sialic acid transport. *Cell.* 39:295–299.
18. Drake, R.R., Y. Igari, R. Lester, A.D. Elbein, and A. Radominska. 1992. Application of 5-azido-UDP-glucose and 5-azido-UDP-glucoronic acid photoaffinity probes for the determination of the active site orientation of microsomal UDP-glucosyltransferases and UDP-glucuronyltransferase. *J. Biol. Chem.* 267:11360–11365.
19. Farrer, R.G., M.P. Warden, and R.H. Quarles. 1995. Effects of brefeldin A on galactosphingolipid synthesis in an immortalized Schwann cell line: evidence for different intracellular locations of galactosylceramide sulfotransferase and ceramide galactosyltransferase activities. *J. Neurochem.* 65:1865–1873.
20. Futerman, A.H., and R.E. Pagano. 1991. Determination of the intracellular sites and topology of glucosylceramide synthesis in rat liver. *Biochem. J.* 280:295–302.
21. Gillard, B.K., L.T. Thurmon, and D.M. Marcus. 1992. Association of glycosphingolipids with intermediate filaments of mesenchymal, epithelial, glial, and muscle cells. *Cell Motil. Cytoskeleton.* 21:255–271.
22. Hammond, C., and A. Helenius. 1994. Quality control in the secretory pathway: retention of a misfolded viral membrane glycoprotein involves cycling between the ER, intermediate compartment, and Golgi apparatus. *J. Cell Biol.* 126:41–52.
23. Hansson, G.C., K. Simons, and G. van Meer. 1986. Two strains of the Madin-Darby canine kidney (MDCK) cell line have distinct glycosphingolipid compositions. *EMBO (Eur. Mol. Biol. Organ.) J.* 5:483–489.
24. Herrmann, A., A. Zachowski, and P.F. Devaux. 1990. Protein-mediated phospholipid translocation in the endoplasmic reticulum with a low lipid specificity. *Biochemistry.* 29:2023–2027.
25. Hirschberg, C.B., and M.D. Snider. 1987. Topography of glycosylation in the rough endoplasmic reticulum and Golgi apparatus. *Annu. Rev. Biochem.* 56:63–87.
26. Hirschberg, K., J. Rodger, and A.H. Futerman. 1993. The long-chain sphingoid base of sphingolipids is acylated at the cytosolic surface of the endoplasmic reticulum in rat liver. *Biochem. J.* 290:751–757.
27. Inokuchi, J., and N.S. Radin. 1987. Preparation of the active isomer of 1-phenyl-2-decanoylamino-3-morpholino-1-propanol, inhibitor of murine glucocerebroside synthetase. *J. Lipid Res.* 28:565–571.
28. Jeckel, D., A. Karrenbauer, K.N.J. Burger, G. van Meer, and F. Wieland. 1992. Glucosylceramide is synthesized at the cytosolic surface of various Golgi subfractions. *J. Cell Biol.* 117:259–267.
29. Kean, E.L. 1966. Separation of gluco- and galactocerebrosides by means of borate thin-layer chromatography. *J. Lipid Res.* 7:449–452.
30. Klausner, R.D., J.G. Donaldson, and J. Lippincott-Schwartz. 1992. Brefeldin A: insights into the control of membrane traffic and organelle structure. *J. Cell Biol.* 116:1071–1080.
31. Kok, J.W., M. ter Beest, G. Scherphof, and D. Hoekstra. 1990. A non-exchangeable fluorescent phospholipid analog as a membrane traffic marker of the endocytic pathway. *Eur. J. Cell Biol.* 53:173–184.
32. Kotani, M., H. Hosoya, H. Kubo, K. Itoh, H. Sakuraba, M. Kusubata, M. Inagaki, K. Yazaki, Y. Suzuki, and T. Tai. 1994. Evidence for direct binding of intracellularly distributed ganglioside GM2 to isolated vimentin intermediate filaments in normal and Tay-Sachs disease human fibroblasts. *Cell Struct. Funct.* 19:81–87.
33. Lannert, H., C. Bünning, D. Jeckel, and F.T. Wieland. 1994. Lactosylceramide is synthesized in the lumen of the Golgi apparatus. *FEBS Lett.* 342:91–96.
34. Louvard, D. 1980. Apical membrane aminopeptidase appears at sites of cell-cell contact in cultured kidney epithelial cells. *Proc. Natl. Acad. Sci. USA.* 77:4132–4136.
35. Mandon, E.C., I. Ehses, J. Rother, G. van Echten, and K. Sandhoff. 1992. Subcellular localization and membrane topology of serine palmitoyltransferase, 3-dehydrosphinganine reductase, and sphinganine N-acyltransferase in mouse liver. *J. Biol. Chem.* 267:11144–11148.
36. Mayer, L.D., M.J. Hope, and P.R. Cullis. 1986. Vesicles of variable sizes produced by a rapid extrusion procedure. *Biochim. Biophys. Acta.* 858:161–168.
37. McIntyre, J.C., and R.G. Sleight. 1991. Fluorescence assay for phospholipid membrane asymmetry. *Biochemistry.* 30:11819–11827.
38. Morell, P., and N.S. Radin. 1969. Synthesis of cerebroside by brain from uridine diphosphate galactose and ceramide containing hydroxy fatty acid. *Biochemistry.* 8:506–512.
39. Niimura, Y., and I. Ishizuka. 1986. Glycosphingolipid composition of a renal cell line (MDCK) and its ouabain-resistant mutant. *J. Biochem.* 100:825–835.
40. Nilsson, T., and G. Warren. 1994. Retention and retrieval in the endoplasmic reticulum and the Golgi apparatus. *Curr. Opin. Cell Biol.* 6:517–521.
41. Pagano, R.E., and O.C. Martin. 1988. A series of fluorescent N-acylsphingosines: synthesis, physical properties, and studies in cultured cells. *Biochemistry.* 27:4439–4445.
42. Perez, M., and C.B. Hirschberg. 1985. Translocation of UDP-N-acetylglucosamine into vesicles derived from rat liver rough endoplasmic reticu-

lum and Golgi apparatus. *J. Biol. Chem.* 260:4671–4678.
43. Rijnboutt, S., H.M. Aerts, H.J. Geuze, J.M. Tager, and G.J. Strous. 1991. Mannose 6-phosphate-independent membrane association of cathepsin D, glucocerebrosidase, and sphingolipid-activating protein in HepG2 cells. *J. Biol. Chem.* 266:4862–4868.
44. Sasaki, T. 1990. Glycolipid transfer protein and intracellular traffic of glucosylceramide. *Experientia.* 46:611–616.
45. Sasaki, T., and R.A. Demel. 1985. Net mass transfer of galactosylceramide facilitated by glycolipid transfer protein from pig brain: a monolayer study. *Biochemistry.* 24:1079–1083.
46. Sato, C., J.A. Black, and R.K. Yu. 1988. Subcellular distribution of UDP-galactose:ceramide galactosyltransferase in rat brain oligodendroglia. *J. Neurochem.* 50:1887–1893.
47. Schaeren-Wiemers, N., P. van der Bijl, and M.E. Schwab. 1995. The UDP-galactose:ceramide galactosyltransferase: expression pattern in oligodendrocytes and Schwann cells during myelination and substrate preference for hydroxyceramide. *J. Neurochem.* 65:2267–2278.
48. Schulte, S., and W. Stoffel. 1993. Ceramide UDPgalactosyltransferase from myelinating rat brain—Purification, cloning, and expression. *Proc. Natl. Acad. Sci. USA.* 90:10265–10269.
49. Schweizer, A., H. Clausen, G. van Meer, and H.P. Hauri. 1994. Localization of O-glycan initiation, sphingomyelin synthesis, and glucosylceramide synthesis in Vero cells with respect to the endoplasmic reticulum-Golgi intermediate compartment. *J. Biol. Chem.* 269:4035–4041.
50. Spitalnik, P.F., J.M. Danley, S.R. Burger, and S.L. Spitalnik. 1989. The glycosphingolipid composition of the human hepatoma cell line, Hep-G2. *Arch. Biochem. Biophys.* 273:578–591.
51. Stahl, N., H. Jurevics, P. Morell, K. Suzuki, and B. Popko. 1994. Isolation, characterization, and expression of cDNA clones that encode rat UDP-galactose: ceramide galactosyltransferase. *J. Neurosci. Res.* 38:234–242.
52. Stanley, P., and L. Siminovitch. 1977. Complementation between mutants of CHO cells resistant to a variety of plant lectins. *Som. Cell Genet.* 3: 391–405.
53. Strous, G.J., P. van Kerkhof, G. van Meer, S. Rijnboutt, and W. Stoorvogel. 1993. Differential effects of Brefeldin-A on transport of secretory and lysosomal proteins. *J. Biol. Chem.* 268:2341–2347.
54. Tennekoon, G., M. Zaruba, and J. Wolinsky. 1983. Topography of cerebroside sulfotransferase in Golgi-enriched vesicles from rat brain. *J. Cell Biol.* 97:1107–1112.
55. Trinchera, M., M. Fabbri, and R. Ghidoni. 1991. Topography of glycosyltransferases involved in the initial glycosylations of gangliosides. *J. Biol. Chem.* 266:20907–20912.
56. Trinchera, M., A. Fiorilli, and R. Ghidoni. 1991. Localization in the Golgi apparatus of rat liver UDP-Gal: glucosylceramide β 1-4galactosyltransferase. *Biochemistry.* 30:2719–2724.
57. van den Besselaar, A.M.H.P., B. de Kruijff, H. van den Bosch, and L.L.M. van Deenen. 1978. Phosphatidylcholine mobility in liver microsomal membranes. *Biochim. Biophys. Acta.* 510:242–255.
58. van der Bijl, P., M. Lopes-Cardozo, and G. van Meer. 1996. Sorting of newly synthesized galactosphingolipids to the two surface domains of epithelial cells. *J. Cell Biol.* 132.
59. van Echten, G., and K. Sandhoff. 1993. Ganglioside metabolism—enzymology, topology, and regulation. *J. Biol. Chem.* 268:5341–5344.
60. van Genderen, I.L., G. van Meer, J.W. Slot, H.J. Geuze, and W.F. Voorhout. 1991. Subcellular localization of Forssman glycolipid in epithelial MDCK cells by immuno-electronmicroscopy after freeze-substitution. *J. Cell Biol.* 115:1009–1019.
61. van Meer, G., and K.N.J. Burger. 1992. Sphingolipid trafficking—sorted out? *Trends Cell Biol.* 2:332–337.
62. van Meer, G., E.H.K. Stelzer, R.W. Wijnaendts-van-Resandt, and K. Simons. 1987. Sorting of sphingolipids in epithelial (Madin-Darby canine kidney) cells. *J. Cell Biol.* 105:1623–1635.
63. Vunnam, R.R., and N.S. Radin. 1979. Short chain ceramides as substrates for glucocerebroside synthetase: differences between liver and brain enzymes. *Biochim. Biophys. Acta.* 573:73–82.
64. Warnock, D.E., M.S. Lutz, W.A. Blackburn, W.W. Young, and J.U. Baenziger. 1994. Transport of newly synthesized glucosylceramide to the plasma membrane by a non-Golgi pathway. *Proc. Natl. Acad. Sci. USA.* 91:2708–2712.
65. Yusuf, H.K.M., G. Pohlentz, and K. Sandhoff. 1983. Tunicamycin inhibits ganglioside biosynthesis in rat liver Golgi apparatus by blocking sugar nucleotide transport across the membrane vesicles. *Proc. Natl. Acad. Sci. USA.* 80:7075–7079.
66. Zilversmit, D.B., and M.E. Hughes. 1977. Extensive exchange of rat liver microsomal phospholipids. *Biochim. Biophys. Acta.* 469:99–110.